Available online at www.sciencedirect.com
SCIENCE DIRECT
Neurotoxicology and Teratology 28 (2006) 220–228
NEUROTOXICOLOGY AND TERATOLOGY
www.elsevier.com/locate/neutera

Relative toxicities and neuromuscular nicotinic receptor agonistic potencies of anabasine enantiomers and anabaseine

Stephen T. Lee [a,*], Kristin Wildeboer [b], Kip E. Panter [a], William R. Kem [b], Dale R. Gardner [a], Russell J. Molyneux [c], Cheng-Wei Tom Chang [d], Ferenc Soti [b], James A. Pfister [a]

[a] *Poisonous Plant Research Laboratory, Agricultural Research Service, United States Department of Agriculture, 1150 E. 1400 N., Logan, UT 84341, USA*
[b] *Department of Pharmacology and Therapeutics, College of Medicine, University of Florida, 1600 S. W. Archer Road, Gainesville, FL 32610-0267, USA*
[c] *Western Regional Research Center, Agricultural Research Service, United States Department of Agriculture, 800 Buchanan Street, Albany, CA 94710, USA*
[d] *Department of Chemistry and Biochemistry, Utah State University, 0300 Old Main Hill, Logan, UT 84322-0300, USA*

Received 16 June 2005; received in revised form 14 December 2005; accepted 15 December 2005
Available online 20 February 2006

Abstract

Anabasine occurring in wild tree tobacco (*Nicotiana glauca*) and anabaseine occurring in certain animal venoms are nicotinic receptor agonist toxins. Anabasine lacks the imine double bond of anabaseine; the two possible enantiomers of anabasine occur in *N. glauca*. A comparision of the relative potencies of *S*- and *R*-anabasine has not been previously reported. We separated the enantiomers of anabasine by reaction of the racemic *N. glauca* natural product with 9-fluorenylmethoxycarbonyl-L-alanine (Fmoc-L-Ala-OH) to give diastereomers, which were separated by preparative reversed phase HPLC. The *S*- and *R*-anabasine enantiomer fractions were then obtained by Edman degradation. A mouse bioassay was used to determine the relative lethalities of *S*- and *R*-enriched anabasine enantiomers. The intravenous LD_{50} of the (+)-*R*-anabasine rich fraction was 11 ± 1.0 mg/kg and that of the (−)-*S*-anabasine-rich fraction was 16 ± 1.0 mg/kg. The LD_{50} of anabaseine was 0.58 ± 0.05 mg/kg. Anabaseine was significantly more toxic in the mouse bioassay than *S*-anabasine (27-fold) and *R*-anabasine (18-fold). The relative agonistic potencies of these three alkaloids on human fetal nicotinic neuromuscular receptors were of the same rank order: anabaseine ≫ *R*-anabasine > *S*-anabasine.

Keywords: Anabasine; Anabaseine; Enantiomer; Nicotinic receptor; Toxicity

1. Introduction

Feeding pregnant cows, gilts, ewes, and goats with ground plant material of the wild tree tobacco *Nicotiana glauca* at specific gestational periods results in calves, piglets, lambs and kids with multiple congenital contractures (MCC) and cleft palates [15–17,32]. Anabasine (1, Fig. 1), as a racemic mixture, has been shown to be the predominant alkaloid in *N. glauca* and has been identified as the responsible teratogen [15]. Research with anabasine-induced fetal cleft palates in pregnant goats has resulted in a congenital caprine model for the study of the etiology of cleft palate and development of improved treatments in children [39–42]. Human ingestion of *N. glauca* leaves causes neuromuscular paralysis and death and this has been attributed to anabasine [29,30,36,37]. Anabasine has also been found in nemertine worms and ants [19,26].

Anabaseine (2, Fig. 1), a compound structurally similar to anabasine, has been proposed to be more toxic and a more potent teratogen than anabasine due to the presence of a double bond between the 1 and 2 positions in the piperidine ring [34]. The greater toxicities of the 1,2-dehydro piperidines relative to the corresponding piperidines have been established for γ-coniceine in poison hemlock (*Conium maculatum*) and *N*-acetylhystrine from piperidine-containing lupines [33]. Anabaseine has not yet been found in plants, but is a toxin used by carnivorous marine worms (hoplonemertines) to paralyze their prey and is the primary compound in the poison glands of *Messor* and *Aphenaenogaster* ants [4,18,21,43]. Anabaseine and *S*-anabasine actions on vertebrate nicotinic receptors have been reported [23]. Also, the mouse toxicity of anabaseine has been compared with that of *S*-nicotine [22]. A compound synthesized from anabaseine is in clinical tests for possible

* Corresponding author. Tel.: +1 435 752 2941; fax: +1 435 753 5681.
E-mail address: stlee@cc.usu.edu (S.T. Lee).

0892-0362/$ - see front matter © 2006 Published by Elsevier Inc.
doi:10.1016/j.ntt.2005.12.010

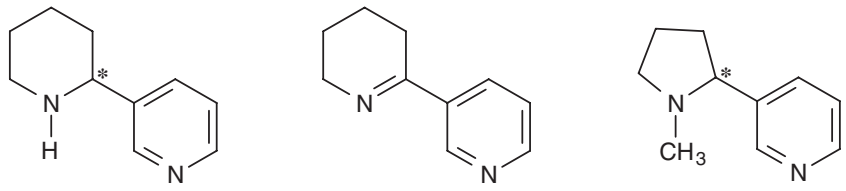

Fig. 1. The chemical structures of anabasine 1, anabaseine 2, and nicotine 3. In anabasine the asymmetric carbon is alpha to the piperidine nitrogen and also is connected to the pyridine ring.

treatment of cognitive deficits in Alzheimer's patients and schizophrenics [20,24,25,28].

Stereochemical integrity is a significant factor in determining the specificity of biological effects of chiral compounds, both in natural products and synthetic compounds [5]. Previously, we reported the separation and isolation of ammodendrine enantiomers from *Lupinus formosus* plant collections [27]. These results led us to investigate the possibility of separating and isolating the anabasine enantiomers reportedly produced by *N. glauca* plants [17]. To separate anabasine, we converted the enantiomers into diastereomers which then allowed the analysis and isolation of the anabasine-based diastereomers by traditional reversed phase HPLC. The separated anabasine diastereomers were subsequently converted to their *R*- and *S*-anabasine fractions. Enantiomers often have very different physiological activities, thus, it was important to measure the relative potencies of the *R*- and *S*-anabasines individually. In our study, the toxicities of the *R*- and *S*-anabasine fractions and the structurally similar anabaseine were measured in a mouse lethality bioassay. Also, the neuromuscular nicotinic receptor (nAChR) agonist potencies of the alkaloids were assessed using a human tumor cell line (TE671) expressing fetal muscle type nAChRs.

2. Materials and methods

2.1. Materials

Acetic acid, ammonium hydroxide, *n*-hexane, *N*,*N*-dimethyl formamide (DMF), and sulfuric acid were obtained from Fisher Scientific (Pittsburgh, PA). Hydroxybenzotriazole, phenyl isothiocyanate (99%), piperidine (99.5%), poly-D-lysine and silica gel (70–230 mesh 60 Å) were purchased from Sigma-Aldrich Chemical Co. (St. Louis, MO and Milwaukee, WI). (L)-Fmoc-L-alanine-OH and *N*-(3-dimethylaminopropyl)-*N*′-ethylcarbodiimide hydrochloride were obtained from Fluka Chemical Corp. (Ronkonkoma, NY). Trifluoroacetic acid was from EM Science (Gibbstown, NJ), anhydrous sodium sulfate from Baker, Inc. (Phillipsburg, NJ), chloroform from Mallinckrodt Baker Inc. (Paris, KY), racemic epibatidine from Tocris (Ellisvile, MD) and ammonium acetate from VWR (Bristol, CT). Anabaseine was synthesized as the dihydrochloride salt monohydrate as previously described [3]. Fetal bovine serum and penicillin/streptomycin were from Media Tech, Inc. (Herndon, VA), Dulbecco's modified Eagle's medium was from the American Type Culture Collection (Manassas, VA), and the fluorescence dye kits were purchased from Molecular Devices (Sunnyvale, CA).

2.2. Analytical techniques

Electrospray mass spectrometric (ESI-MS) data were acquired on a LCQ mass spectrometer (Finnigan Corporation, San Jose, CA). Samples were loop injected into the ESI source using a methanol : 20 mM ammonium acetate solution, 50 : 50 v/v, at a flow rate of 0.5 mL/min. The ESI ion source was operated with a capillary temperature of 250 °C, capillary voltage 36 V, spray voltage 4.5 kV, sheath gas flow rate 70 U and, auxiliary gas flow rate 20 U. The mass spectrometer scanned the mass range of 100–800 amu in positive ion mode. High resolution mass spectrometry (HRESI) was provided by the Washington University Mass Spectrometry Resource (St Louis. MO). Acetonitrile : water 1 : 1 was used as solvent, and sodium trifluoroacetate was used as standard. Log #s for the compounds analyzed by HRESI and reported herein are 16455, 16456, and 16457. Optical rotations were recorded on a Perkin–Elmer model 241 polarimeter.

2.2.1. Analytical scale reversed phase HPLC

Racemic anabasine and chiral isolates were derivatized by the procedure in Section 2.4 to form L-Fmoc-Ala-anabasine and analyzed by analytical scale HPLC using a 100 mm × 2 mm i.d., 5 μm Betasil C-18 column (Thermo Hypersil-Keystone, Bellefonte, PA). The mobile phase was 20 mM ammonium acetate/methanol (45 : 55, v/v) at a flow rate of 0.5 mL/min. The detector was a Finnigan LCQ mass spectrometer operating in ESI mode.

2.2.2. Semi-preparative scale reversed phase HPLC

The Ala-anabasine diastereomers were separated and isolated using a semi-preparative scale 250 mm × 10 mm i.d., 5 μm, Betasil C-18 HPLC column (Thermo Hypersil–Keystone, Bellefonte, PA). The mobile phase was 20 mM ammonium acetate : methanol (80 : 20, v/v) at a flow rate of 5 mL/min. The detector was a Waters 486 UV–vis absorbance detector (Waters Corporation, Milford, MA) operating at 220 nm.

2.2.3. Analytical scale chiral HPLC

Microgram quantities of the *S*- and *R*-anabasine samples used in the toxicity and functional nicotinic receptor

experiments were analyzed using an analytical column 250 mm × 4.6 mm i.d., Daicel chiral OJ-H purchased from Chiral Technologies, Inc. (Exton, PA). The column was equilibrated and eluted with *n*-hexane/ethanol/diethylamine/-trifluoroacetic acid (97:3:0.1:0.1, v/v/v/v) at a flow rate of 1 mL/min. The compounds were run on a Beckman Gold Nouveau HPLC instrument equipped with a photodiode array detector; peaks were measured at 260 nm.

2.3. Collection and isolation of alkaloids from wild tobacco

N. glauca plant material was collected near Kingman, Arizona in early June 2004, air dried, ground in a hammer mill to pass through a 2 mm screen, and stored at ambient temperature. Anabasine was extracted and isolated as previously described [17].

2.4. Synthesis and separation of anabasine diastereomers

Anabasine, (107.4 mg, 0.6620 mmol), L-Fmoc-Ala-OH (285.2 mg, 0.8660 mmol), *N*-(3-dimethylaminopropyl)-*N*′-ethylcarbodiimide hydrochloride (166.3 mg, 0.8675 mmol) and hydroxybenzotriazole (158.4 mg, 1.172 mmol) were weighed into a round bottom flask (10 mL) and *N*,*N*-dimethylformamide (DMF) (7 mL) was added. The reaction was carried out under a N_2 atmosphere and stirred with a magnetic stirbar at room temperature (RT) for 16 h. The DMF was evaporated off with compressed air, the reaction mixture dissolved in $CHCl_3$ and the organic layer washed (2×) with distilled deionized water. The $CHCl_3$ phase was then dried over sodium sulfate, filtered and rotary evaporated to an oily residue. The residue was sampled by ESI-MS and the mass spectrum indicated that much of the anabasine had reacted to form L-Fmoc-Ala-anabasine, ($MH^+ = 456$). Based on analytical scale reversed phase HPLC-MS analysis (Section 2.2.1), approximately 50% of the anabasine had been consumed to form L-Fmoc-Ala-anabasine. High resolution ESI-MS (*m*/*z*): $[M+H]^+$calcd for $C_{28}H_{30}0_9N_3O_3$, 456.2287; found, 456.2279.

The Fmoc portion of L-Fmoc-Ala-anabasine was removed by reaction with a 25% solution of piperidine (1 mL) in methylene chloride (3 mL) for 1 h at room temperature. The reaction mixture was dried with a gentle flow of N_2 at 65 °C. The reaction mixture was dissolved in 1% H_2SO_4 and $CHCl_3$ and the aqueous layer was washed (3×) with $CHCl_3$ and then made basic to pH 9 with NH_4OH. The basic aqueous layer was then extracted (3×) with $CHCl_3$. The $CHCl_3$ extracts were combined, dried with anhydrous Na_2SO_4, filtered, and rotary evaporated to dryness. The residue was sampled by flow injection ESI-MS. The mass spectrum indicated the residue was Ala-anabasine ($MH^+ = 234$) and that this reaction had proceeded to completion as Fmoc-Ala-anabasine was not present in the mass spectrum. High resolution ESI-MS (*m*/*z*): $[M+H]^+$calcd for $C_{13}H_{19}N_3O$, 234.1606; found, 234.1600.

The Ala-anabasine diastereomers were separated and isolated using the semi-preparative reversed phase HPLC method described in Section 2.2.2. Each of the two major peaks were separately collected and combined with the corresponding peak on subsequent runs. The mobile phase was evaporated to <500 mL and made basic to pH 9 with NH_4OH. The basic aqueous solution was then extracted with equal volumes of chloroform (3×). The $CHCl_3$ extracts were combined, dried with anhydrous Na_2SO_4, filtered, and rotary evaporated to dryness.

2.5. Edman degradation

The L-alanine portion of each Ala-anabasine diastereomer was removed via Edman degradation. The Ala-anabasine diastereomer from the first eluting peak (peak 1, 87.6 mg, 0.374 mmol) and the Ala-anabasine diastereomer from the second eluting peak (peak 2, 75.6 mg, 0.324 mmol) were each treated separately with 5 mL methanol/water/triethylamine/phenylisothiocyanate (3.5:0.5:0.5:0.5, v/v/v/v) solution while stirring at 50 °C. After 1.5 h, trifluoroacetic acid (0.5 mL) was added and the reactions stirred again at 50 °C for an additional 1.5 h. The solvents from the reactions were evaporated under a stream of N_2 at 35 °C. Each reaction mixture was dissolved in 1% H_2SO_4 and extracted with $CHCl_3$ (3×). The aqueous phase was then made basic to pH 9 by addition of NH_4OH. The basic aqueous phase was extracted with $CHCl_3$ (3×) and these organic extracts combined, dried over anhydrous sodium sulfate, filtered, and rotary evaporated to dryness. The residues were sampled by ESI-MS. Mass spectrometric analysis indicated that the major portion of each residue was anabasine ($MH^+ = 163$). Each anabasine enantiomer was isolated by chromatography on a 40 cm × 2.3 cm silica gel column using a mobile phase of $CHCl_3/MeOH/NH_4OH$ (65:35:l, v/v/v). Finally, the enantiomers were cleaned by an acid/base extraction using 1% aqueous H_2SO_4 and extracting with $CHCl_3$. These acidic $CHCl_3$ fractions were discarded. The aqueous portion was then made basic to pH 9 with the addition of NH_4OH and extracted with $CHCl_3$. The basic $CHCl_3$ fractions of a particular enantiomer were combined, dried with anhydrous Na_2SO_4, filtered, and rotary evaporated to dryness to give the anabasine enantiomers (peak 1, 30.5 mg, 0.188 mmol yield, 50.1%; peak 2, 38.4 mg, yield 73.1%).

2.6. Mouse toxicity determinations

Known amounts of the individual alkaloids were dissolved in physiological buffered saline solution. The solutions were stored in sterile injection vials for toxicity testing. Weanling White Swiss–Webster male mice, 15 to 20 g (Simonsen Labs, Gilroy, CA) were weighed after a 12 h fast and dosed intravenously. Injections were performed via the tail vein in mice restrained in a plastic mouse block. Prior to injection, the mice were maintained under a heat lamp for 15 min to dilate the tail vein. The tail vein was cleaned with 70% ethanol and i.v. injections were accomplished with a tuberculin syringe equipped with a 1.27-cm long 27-gauge needle. The volume injected varied depending on the dosage delivered. Time of injection, clinical effects, and time of death were noted and recorded. Mice were closely observed for 1 h after injection. Onset of clinical signs was immediate, beginning with

piloerection, tail flicking and rapidly progressing to intention tremors, clonic convulsions, muscular weakness, lateral recumbency and death. Typically, death occurred within 5 min of injection or recovery was imminent and complete within 1 h. The LD_{50} for individual alkaloid toxicity was determined by a modified up-and-down method [6] and was calculated using the PROC PROBIT procedures of SAS (SAS Institute Inc., Cary, NC) on a logistic distribution of the survival data. Confidence (fiducial) intervals (95%) were also calculated using the same program.

2.7. Nicotinic agonist actions on the fetal human nAChR

Cells expressing the fetal human muscle type nAChR were obtained from Dr. John Daly at NIH and their membrane depolarization responses to sudden application of a nicotinic agonist toxin were measured by changes in fluorescence of a membrane potential-sensitive dye [11]. The TE671 cells were maintained in a culture medium consisting of Dulbecco's modified Eagle's medium supplemented with 10% fetal bovine serum, 100 U/mL penicillin and 100 μg/mL streptomycin and grown in 75 cm^2 culture flasks housed in a humidified incubator at 37 °C in an atmosphere of 5% CO_2. Cells were grown to near confluence before being split at a subcultivation ratio of between 1 : 6 and 1 : 40 weekly. They were seeded at a density of roughly $3–6 \times 10^4$ cells/well into 96-well clear-bottom black-walled culture plates that had been coated with 50 μL per well of 50 μg/mL poly-D-lysine (70–150 kDa) and grown to near confluence overnight in 75 μL of culture medium. The membrane potential dye solution was prepared by dissolving the dried dye within one vial of the Molecular Devices dye into 36 mL Hanks' balanced salt solution (HBSS) supplemented with 20 mM Hepes (pH 7.4). The 96-well cell culture plates were equilibrated to room temperature for 10 min, then the cells were washed once with 100 μL HBSS/Hepes before adding 30 μL of the membrane potential dye solution to each well. The cells were incubated with the dye at room temperature for 45 min before agonist addition and recording. Serial dilutions of a compound for concentration–response analysis were prepared in 96-well V-bottom plates by addition of the required volume of a methanolic stock solution. After evaporation of the methanol, the compound in each well was redissolved in HBSS/Hepes (pH 7.4).

Fluid (agonist or KCl) additions and membrane potential measurements were performed using a Flexstation fluorimeter (Molecular Devices). Excitation and emission wavelengths were set to 530 and 565 nm, respectively; the cut-off wavelength was 550 nm. The proprietary dye is a lipophilic anionic bis-oxonol. When the cells are depolarized it enters the cells and binds to cytosolic proteins, and there is an increase in fluorescence. A reading was taken every 1.44 s for 200 s, a total of 139 readings per well. The first 16 s were used as a basal reading. At 17 s 30 μL of a test compound was added to assess agonist activity. A 30 μL pulse of concentrated KCl in saline was added at 120 s to attain a final concentration of 40 mM KCl in the saline bathing the cells, to serve as a depolarizing calibrant and to correct for interwell differences in dye loading and cell count. Responses were calculated as equal to: $(F_{Max}(\text{Compound}) - F_{Basal})/(F_{Max}(\text{Calibrant}) - F_{Basal})$.

Depolarizing responses to agonists were normalized to the maximum response generated by (±)-epibatidine and fitted to a four parameter logistic equation and graphed with Prism (GraphPad) to determine IC_{50} (inverse of potency), efficacy (maximal degree of activation) and Hill coefficients (maximal slope).

2.8. Nicotinic agonists to rat brain alpha7 and alpha4beta2 receptors

Receptor radioligand binding assays: Binding of *S*- and R-anabasine samples to rat brain alpha7 and alpha4beta2 receptors was measured by displacement of (^{125}I)-alpha-bungarotoxin

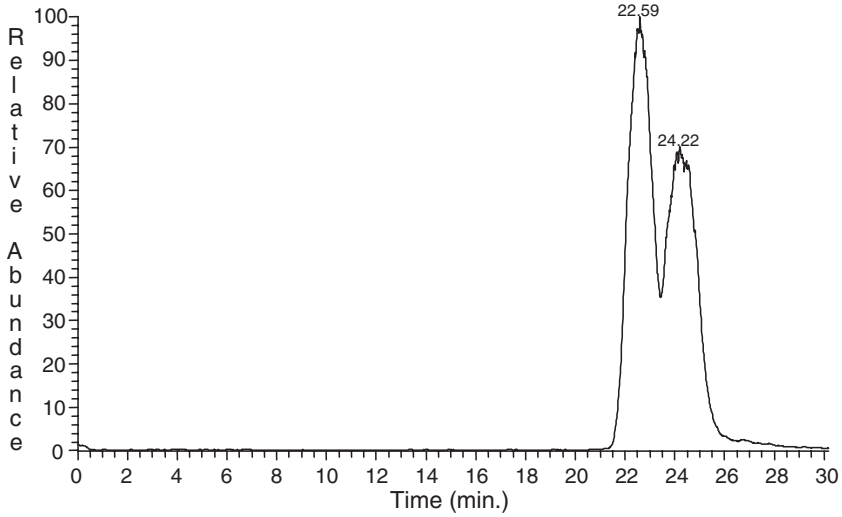

Fig. 2. Reconstructed HPLC ion chromatogram (*m/z* 456.3) for Fmoc-L-Ala-anabasine based diastereomers from *N. glauca* obtained by reversed phase HPLC using a 100 mm × 2 mm i.d., 5 μm Betasil C-18 column with a mobile phase of 20 mM ammonium acetate/methanol (45 : 55, v/v) at a flow rate of 0.5 mL/min. The detector was a Finnigan LCQ mass spectrometer operating in ESI mode.

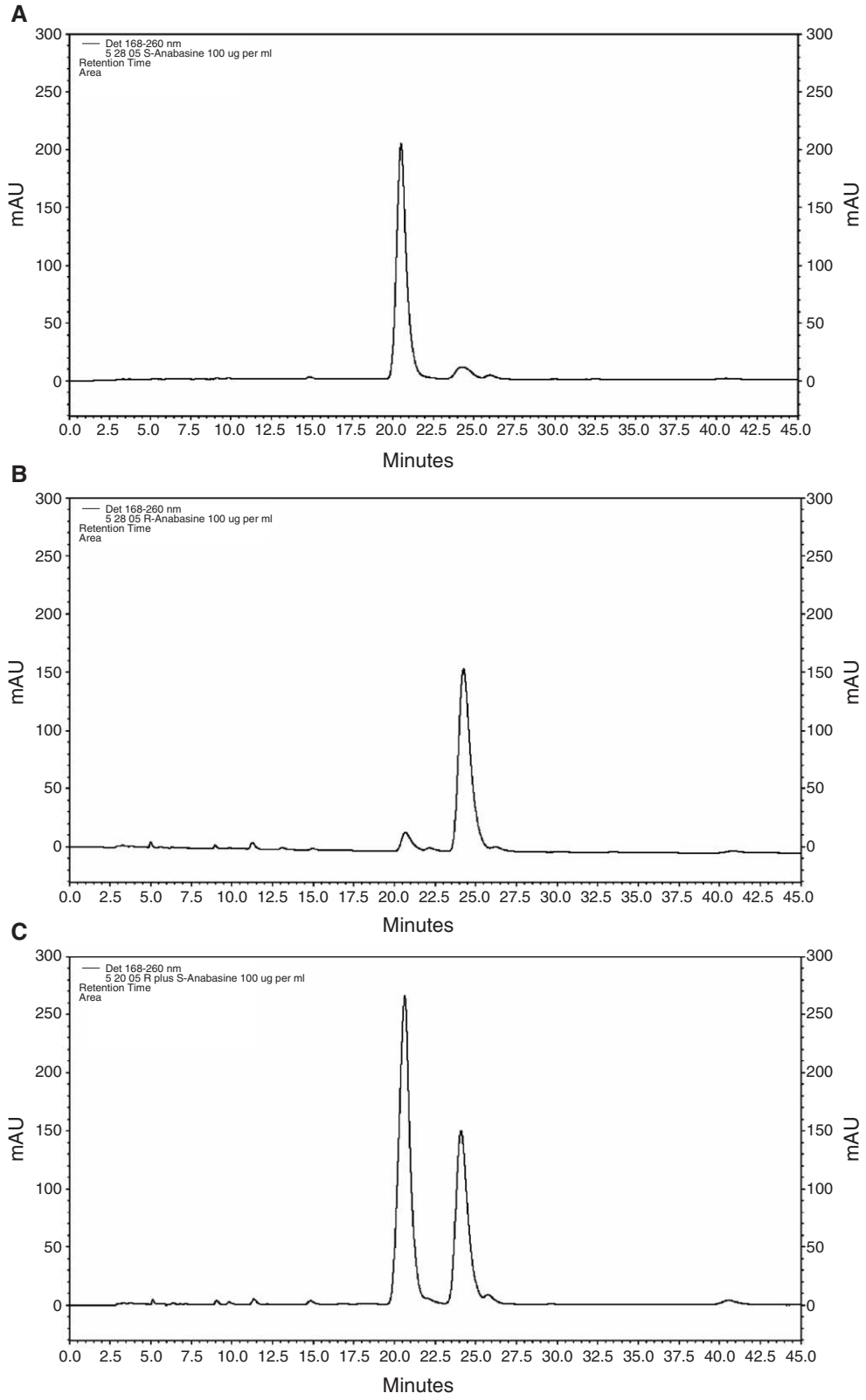

Fig. 3. Chiral HPLC analysis of the two anabasine enantiomer fractions obtained by separation of the Fmoc-Ala-coupled diastereomers, after their subsequent cleavage to yield anabasine. In A, the *S*-enriched fraction is separated; in B, the *R*-enriched anabasine fraction, and in C equal volumes of the two fractions were co-injected. Commercially available *S*-anabasine was also shown to elute with a retention time corresponding to the *S*-enriched fraction major peak. The chromatography was performed using a 250 mm × 4.6 mm i.d., Daicel chiral OJ-H column with a *n*-hexane/ethanol/diethylamine/-trifluoroacetic acid (97 : 3 : 0.1 : 0.1, v/v/v/v) mobile phase at a flow rate of 1 mL/min.The compounds were detected with a UV–vis diode array detector at 260 nm.

and (^{3}H)-cytisine binding, respectively, according to Kem et al. [24].

3. Results

Anabasine was extracted and isolated from *N. glauca* plant material. The above-ground tobacco plant material was analyzed for anabasine using a flow injection ESI-MS procedure and was measured to be 0.55% of the composite dry weight. We converted the anabasine enantiomers into diastereomers by a peptide coupling reaction where anabasine was reacted with Fmoc-L-Ala-OH in the presence of *N*-(3-dimethylaminopropyl)-*N*′-ethylcarbodiimide hydrochloride and hydroxybenzotriazole dissolved in *N*,*N*-dimethyl formamide (DMF). The progress of the reaction was monitored by ESI-MS. The mass spectra indicated the formation of Fmoc-L-Ala-anabasine, (MH^+ = 456). Fig. 2 shows that the diastereomers can be separated by reversed phase HPLC described in Section 2.2.1 and confirms that both anabasine enantiomers were present in the *N. glauca* plant material.

Removal of the Fmoc moiety was performed by reaction of Fmoc-L-Ala-anabasine with piperidine in methylene chloride. ESI-MS indicated that the reaction product was L-Ala-anabasine, (MH^+ 234). The semi-preparative reversed phase HPLC method described in Section 2.2.2 was used to isolate milligram quantities of the two L-Ala-anabasine diastereomers. Conversion of the isolated diasteriomers to their respective enantiomeric forms of anabasine was then accomplished by an Edman degradation procedure to remove the L-alanine. The progress of the reaction was monitored by ESI-MS, which indicated that the major portion of the reaction residue was anabasine, (MH^+ 163). The *R*- and *S*-anabasine fractions were separated from the reaction mixture by conventional silica gel column chromatography. *R*- and *S*-anabasine aliquots (<5 mg) were reacted with Fmoc-L-Ala-OH in the peptide coupling reaction described previously to form L-Fmoc-Ala-anabasine diastereomers. These diastereomers were analyzed using the analytical scale reversed phase HPLC method described in Section 2.2.1. The purity of the *S*-anabasine was 89% and the *R*-anabasine 78% with respect to contamination from the complementary isomer with this HPLC analysis.

The optical rotation of *S*-anabasine has been reported as $[\alpha]_D$ −84° [8], −79.2° [12] and −80° [10]. The optical rotation of our *S*-anabasine fraction was measured as $[\alpha]^{24}_D$ −48.1° and of our *R*-anabasine fraction as $[\alpha]^{22}_D$ +35.5°. Using the optical rotation measurements from our fractions and assuming the optical rotation of anabasine is $[\alpha]_D$ −80°, the purity of the *S*-anabasine enantiomer was calculated to be 80% and that of the *R*-anabasine enantiomer as 72% pure with respect to contamination from the complementary isomer.

The *S*- and *R*-anabasine enantiomers could also be separated by analytical scale chiral HPLC (Section 2.2.3; Fig. 3). This reported chiral separation of the two anabasine enantiomers encourages us to use this chromatographic method to investigate the enantiomeric compositions of related plant and animal alkaloids which possess asymmetric carbons.

The toxicities of the anabasine enantiomers and anabaseine were compared using a mouse bioassay. The rank order of toxicity was anabaseine (0.58±0.05 mg/kg) ≫ *R*-anabasine (11±1 mg/kg) > *S*-anabasine (16±1 mg/kg) Table 1. This is compared to the previously published toxicities of the enantiomers of nicotine where the *S* enantiomer (0.38±0.06 mg/kg) was more toxic than the *R* enantiomer (2.8±0.9) [1]. To facilitate the comparison of the pharmacological properties of anabaseine and the *S*- and *R*-anabasine samples, the neuromuscular nAChR agonist potencies of the three compounds were determined on a cell line expressing a fetal form of the human neuromuscular nAChR. Also the ability of the compounds to bind to the major brain nAChRs (alpha4beta2 and alpha7) was determined. These data are shown in Table 1. Functional as well as radioligand binding data from a previous analysis of anabaseine, nicotine and *S*-anabasine are included for comparison [23].

Table 1
Pharmacological properties of the three related nAChR agonists and (*S*)-nicotine (for comparison)

Compound	Anabaseine	Nicotine	Anabasine	
		(*S*)-	(*S*)-	(*R*)-
LD_{50} (mg/kg)	0.58±0.05	0.38±0.06 [a]	16±1.0	11±1.0
Human fetal muscle nAChR				
EC_{50} (μM)	0.42±0.079	26±4.9	7.1±1.3	2.6±0.56
Max. (%)	97±6.4	79±1.6	101±9.1	97±6.9
Rat alpha7 nAChR				
EC_{50} (μM)	18±1.5 [b]	62±8.9 [b]	18±4.0 [b]	ND
Efficacy (% max.)	100 [b]	63 [b]	100 [b]	ND
Binding K_i (μM)	0.17±0.021 [b]	0.56±0.49 [b]	0.39±0.086	3.7±1.4
Rat alpha4beta2				
EC_{50} (μM)	12±3.8 [b]	19±9.9 [b]	>30 [b]	ND
Efficacy (% max.)	8 [b]	40 [b]	2 [b]	ND
Binding K_i (μM)	0.094±0.011 [b]	0.0056±0.0014 [b] 0.014±0.0004 [c]	1.1±0.11	0.91±0.32

ND = not determined.
[a] [1] (*R*-nicotine LD_{50} was 2.8±0.9 mg/kg).
[b] [23].
[c] [7] (*R*-nicotine K_i was 0.10±0.005 μM).

4. Discussion

Epidemiology studies in the late 1960s and early 1970s showed a high incidence of skeletal defects and cleft palate in piglets associated with ingestion of tobacco stalks (*Nicotiana tabaccum*) by sows early in pregnancy [9]. Subsequent feeding trials in pregnant sows with tobacco leaves, tobacco stalks and purified alkaloids determined that anabasine was the teratogen not nicotine [17]. While nicotine was the predominant alkaloid in the leaves, anabasine was relatively high in the tobacco stalks and was the cause of the birth defects in the epidemiology studies. Subsequent pen studies on cows, sheep, pigs, and goats where purified anabasine or plant (*N. glauca*), where anabasine was the predominant alkaloid (98%), confirmed anabasine as the teratogenic alkaloid in *N. tabaccum* [15–17,32]. Studies using a goat model and ultrasound imaging determined that fetal activity is reduced or eliminated when the mother goat is fed anabasine or *N. glauca* [32]. We hypothesize that when the pregnant mother goat is fed anabasine or *N. glauca* this anabasine-induced fetal paralysis results from neuromuscular blockade and is responsible for both cleft palate and skeletal contracture defects in the newborn [31,32,34].

In 1978, Keeler and Balls evaluated the teratogenic activity of *Conium* alkaloids and analogs and predicted that piperidine alkaloids with specific structural characteristics would be teratogenic [14]. These structural characteristics included a piperidine ring and a side chain of three carbons or larger alpha to the nitrogen in the piperidine ring. Panter et al. further predicted that a double bond between the nitrogen and the alpha carbon in the piperidine ring would enhance teratogenic potency (see Fig. 1 for a comparison of anabasine and anabaseine) [34]. This theory is supported by the rank order of toxicity in the mouse bioassay and the effects on the human fetal muscle nAChR (anabaseine ≫ *R*-anabasine > *S*-anabasine) reported herein. In addition, a study of the in vitro properties of anabaseine and *S*-anabasine found that the potency of anabaseine for contracting frog skeletal muscle was approximately 10-fold higher than for anabasine [23].

Baldwin and Racowshy studied the effect of nicotine and cotinine on the two-cell mouse embryo and found no effect at the level expected in the average smoker (0.4 to 4 μM) [2]. Concentration of nicotine at or below 0.5 mM and concentrations of cotinine at or below 0.008 mM did not adversely affect development. Ignatieva et al. reported adverse effects on germ cells produced by nicotine, administered to rats from the first through 21 days of pregnancy [13]. Sheveleva administered nicotine in a total dose 0.4–1.5 or 5 mg per kg in rats in different periods of pregnancy [35]. The result was retardation of placental development and alteration of its permeability. There were many cases of embryonic death, the cranio-caudal size and the body mass of fetuses decreased, fetal hemorrhage and developmental disturbances in the cardiovascular system were observed. The differences between the teratogenic effects of anabasine and of nicotine induced defects in the pig studies and other more recent

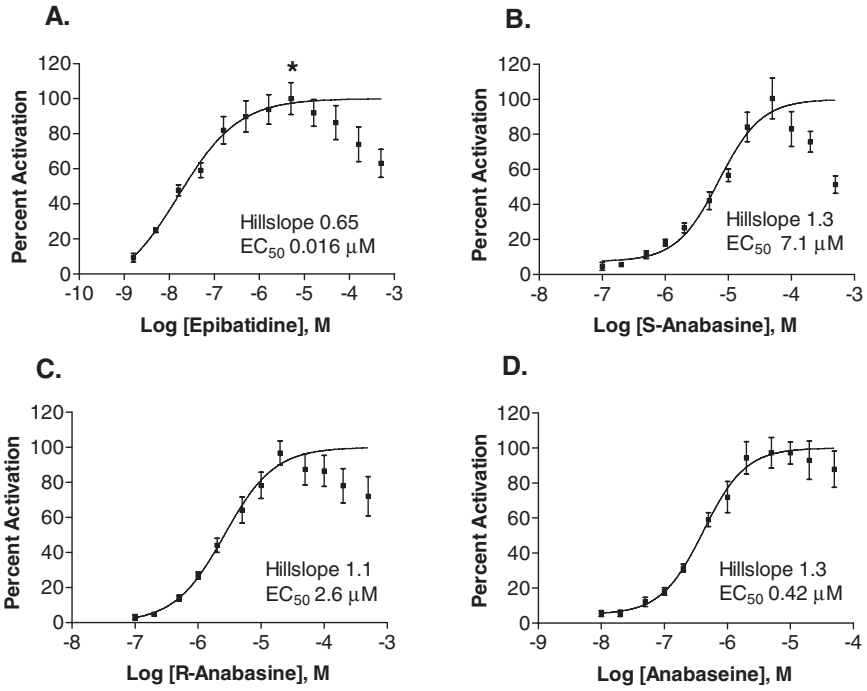

Fig. 4. Functional comparison of the nicotinic receptor activating properties of the two anabasine enantiomer fractions and of anabaseine relative to the most potent known nAChR agonist epibatidine. In each experiment TE671 cells were grown on 96-well black-walled culture plates, and the membrane depolarization resulting from addition of either epibatidine (A), *S*-anabasine (B), *R*-anabasine (C), or anabaseine (D) was measured and calculated as a percentage of the maximal epibatidine response, noted by an asterisk. In each of the four experiments there were duplicate wells. The Hill slope and EC_{50} estimates were calculated using Prism software. Because desensitization occurred at the highest concentrations tested and there is no accepted method for correcting for it, the curves in this figure were obtained by fitting all concentration points up to and including the one producing the largest response and making that response equal to the 100% activation maximum.

studies suggest the teratogenic mechanisms of anabasine and nicotine may be different.

Comparison of the functional and receptor binding properties of anabaseine, *S*- and *R*-anabasines and nicotine (Table 1) further suggests that, while the low LD_{50} of nicotine in the mouse bioassay is most likely related to its central convulsant action, the lethal potencies of anabaseine and the anabasine enantiomers are more likely to be explained by their peripheral actions such as skeletal muscle stimulation and subsequent block. For example anabaseine and *S*-anabasine have essentially little or no stimulatory activity (efficacy) on the alpha4beta2 neuronal receptors through which nicotine is considered to produce convulsions and death (Table 1) [23]. However, anabaseine and anabasine are full agonists on the alpha 7 neuronal receptors. Conversely, nicotine displays low potency for stimulating skeletal muscle type receptors including the fetal type. The relatively high lethal potency of anabaseine due to its peripheral actions is further suggested by the reported similar (i. v. LD_{50}=0.5 mg/kg for Porton, UK strain white mice) lethal potency of a permanently charged analog of anabaseine (2-(3-pyridyl)-3,4,5,6-tetrahydropyridine), which would not be expected to significantly enter the brain, especially during the first few minutes after injection when lethality occurred [38]. Additional evidence that lethality of the anabaseine and the anabasine enantiomers is primarily due to their peripheral neuromuscular actions is that the rank order of lethality (anabaseine ≫ *R*-anabasine > *S*-anabasine) is in rather close agreement with the rank order of potency (EC_{50}) for activation of the fetal skeletal muscle nicotinic receptor (Fig. 4).

It is recognized that acute mouse toxicity is not a surrogate for teratogenicity. However, the structure-activity relationship for toxicity and teratogenicity of related piperidine alkaloids and the significant differences in toxicity and differences in activity on the human fetal muscle nAChR by anabaseine, *R*-anabasine, and *S*-anabasine would suggest that there may be significant differences in the teratogenic potentials of these compounds. If the teratogenic effects of these three alkaloids are due to their ability to cause sustained contracture of the skeletal muscles of the neck and back of the embryo, one would predict, assuming similar pharmacokinetic properties, that the rank order of teratogenic potency would be anabaseine ≫ *R*-anabasine > *S*-anabasine. Additional experiments are in progress to obtain sufficient quantities of each enantiomer and anabaseine to determine the relative teratogenicities of these compounds in a mammalian model.

Acknowledgements

The protocol for animal use in this research was reviewed and approved by the Institutional Animal Care and Use Committee (IACUC), Utah State University, Logan, Utah. We wish to thank J. Christopherson for technical assistance and J. Jacobsen for assistance in plant collection. High resolution mass spectrometry was provided by the Washington University Mass Spectrometry Resource, an NIH Research Resource (Grant No. P41RR0954). The University of Florida (WRK lab) research was supported by NIH RO1-MH6142.

References

[1] M.D. Aceto, B.R. Martin, I.M. Uwaydah, E.L. May, L.S. Harris, C. Izazola-Condo, W.L. Dewey, T.J. Bradshaw, W.C. Vincek, Optically pure (+)-nicotine and biological comparisons with (−) nicotine, J. Med. Chem. 22 (1979) 174–180.
[2] K.V. Baldwin, C. Racowshy, Nicotine and cotinine effects on development of two-cell mouse embryos in vitro, Reprod. Toxicol. 3 (1988) 173–178.
[3] L.B. Bloom, Influence of solvent on the ring-chain hydrolysis equilibrium of anabaseine and syntheses of anabaseine and nicotine analogues. PhD Dissertation, Gainesville, Univ. Florida, 1990, pp. 1–206.
[4] J.M. Brand, S.P. Mpuru, Dufour's gland and poison gland chemistry of the myrmicine ant, *Messor capensis* (Mayr), J. Chem. Ecol. 19 (1993) 1315–1321.
[5] A. Brossi, Chiral drugs: synopsis, Med. Res. Rev. 14 (1994) 665–691.
[6] R. Bruce, An up-and-down procedure for acute toxicity testing, Fundam. Appl. Toxicol. 8 (1987) 97–101.
[7] J.R. Copeland, A. Adem, P. Jacob III, A. Nordberg, A comparison of the binding of nicotine and nornicotine sterioisomers to nicotinic binding sites in rat brain cortex. Nauyn–Schmied, Arch. Pharm. 343 (1991) 123–127.
[8] J.C. Craig, S.K. Roy, Optical rotatory dispersion and absolute configuration-III pyrrolidine, piperdine and tetrahydroisoquinoline alkaloids, Tetrahedron 21 (1965) 401–406.
[9] M.W. Crow, T.W. Swerczek, Congenital arthrogryposis in offspring of sows fed tobacco (*Nicotiana tabacum*), Am. J. Vet. Res. 35 (1974) 1071–1073.
[10] F.X. Felpin, S. Girard, G. VoThanh, R.J. Robins, J. Villierras, J. Lebreton, Efficient enantiomeric synthesis of pyrrolidine and piperidine alkaloids from tobacco, J. Org. Chem. 66 (2001) 6305–6312.
[11] R.W. Fitch, Xiao, K.J. Kellar, J.W. Daly, Membrane potential fluorescence: a rapid and highly sensitive assay for nicotinic receptor channel function, Proc. Natl. Acad. Sci. U. S. A 100 (2003) 4909–4914.
[12] K. Hattori, H. Yamamoto, Asymmetric aza-Diels-Alder reaction mediated by chiral boron reagent, J. Org. Chem. 57 (1992) 3264–3265.
[13] E.L. Ignatieva, L.F. Kurilo, G.L. Mardanova, G.A. Sheveleva, Adverse effects of nicotine on sexual cells of female fetus in rats, Tsitol. Genet. (USSR) 2 (1987) 91–94.
[14] R.F. Keeler, L.D. Balls, Teratogenic effects in cattle of *Conium maculatum* and *Conium* alkaloids and analogs, Clin. Toxicol. 12 (1978) 49–64.
[15] R.F. Keeler, M.W. Crowe, Teratogenicity and toxicology of wild tree tobacco, *Nicotiana glauca* in sheep, Cornell Vet. 74 (1984) 50–59.
[16] R.F. Keeler, J.L. Shupe, M.W. Crowe, J.A. Olson, L.D. Balls, *Nicotiana glauca*-induced congenital deformities in calves: clinical and pathological aspects, Am. J. Vet. Res. 42 (1981) 1231–1234.
[17] R.F. Keeler, M.W. Crowe, E.A. Lambert, Teratogenicity in swine of the tobacco alkaloid anabasine isolated from *Nicotiana glauca*, Teratology 30 (1984) 61–69.
[18] W.R. Kem, A study of the occurrence of anabaseine in *Paranemertes* and other nemertines, Toxicon 9 (1971) 23–32.
[19] W.R. Kem, Pyridine alkaloid distribution in the hoplonemertines, Hydrobiology 156 (1988) 145–151.
[20] W.R. Kem, The brain alpha7 nicotinic receptor may be an important therapeutic target for the treatment of Alzheimer's disease: studies with DMXBA (GTS-21), Behav. Brain Res. 113 (2000) 169–181.
[21] W.R. Kem, B.C. Abbott, R.M. Coates, Isolation and structure of a hoponemertine toxin, Toxicon 9 (1971) 15–22.
[22] W.R. Kem, K.N. Scott, J.H. Duncan, Hoplonemertine worms—a new source of pyridine neurotoxins, Experientia 32 (1976) 684–686.
[23] W.R. Kem, V.M. Mahnir, R.L. Papke, C.J. Lingle, Anabaseine is a potent agonist on muscle and neuronal alpha-bungarotoxin-sensitive nicotinic receptors, J. Pharmacol. Exp. Ther. 283 (1997) 979–992.
[24] W.R. Kem, V.M. Mahnir, L. Prokai, R.L. Papke, X. Cao, S. LeFrancois, K. Wildeboer, K. Prokai-Tatrai, J. Porter-Papke, F. Soti, Hydroxy metabolites of the Alzheimer's drug candidate 3-[2,4-dimethoxy)benzylidene]-anabaseine dihydrochloride (GTS-21): their molecular properties, interactions with brain nicotinic receptors, and brain penetration, Mol. Pharmacol. 287 (2004) 56–67.

[25] H. Kitagawa, T. Takenouchi, R. Azuma, K.A. Wesnes, W.G. Kramer, D.E. Clody, A.L. Burnett, Safety, pharmacokinetics and effects on cognitive function of multiple doses of GTS-21 in healthy, male volunteers, Neuropsychopharmacology 28 (2003) 542–551.
[26] S. LeClercq, S. Charles, D. Daloze, J.-C. Braekman, S. Aron, J.M. Pasteels, Absolute configuration of anabasine from *Messor* and *Aphaenogaster* ants, J. Chem. Ecol. 27 (2001) 945–952.
[27] S.T. Lee, R.J. Molyneux, K.E. Panter, C.W.T. Chang, D.R. Gardner, J.A. Pfister, M. Garrossian, Ammodendrine and *N*-methylammodendrine enantiomers: isolation, optical rotation, and toxicity, J. Nat. Prod. 68 (2005) 681–685.
[28] L.F. Martin, W.R. Kem, R. Freedman, Alpha-7 nicotinic receptor agonists: potential new candidates for the treatment of schizophrenia, Psychopharmacology 174 (2004) 54–64.
[29] L.B. Mellick, T. Makowski, G.A. Mellick, R. Borger, Neuromuscular blockade after ingestion of tree tobacco (*Nicotiana glauca*), Ann. Emerg. Med. 34 (1999) 101–104.
[30] N. Mizrachi, S. Levy, Z.Q. Goren, Fatal poisoning from *Nicotiana glauca* leaves: identification of anabasine by gas-chromatography/mass spectrometry, J. Forensic Sci. 45 (2000) 736–741.
[31] K.E. Panter, R.F. Keeler, Induction of cleft palate in goats by *Nicotiana glauca* during an narrow gestational period and the relation to reduction in fetal movement, J. Nat. Toxins 1 (1992) 25–32.
[32] K.E. Panter, T.D. Bunch, R.F. Keeler, D.V. Sisson, R.J. Callan, Multiple congenital contractures (MCC) and cleft palate induced in goats by ingestion of piperidine alkaloid-containing plants: reduction in fetal movement as the probable cause, J. Toxicol. Clin. Toxicol. 28 (1990) 69–83.
[33] K.E. Panter, D.R. Gardner, R.J. Molyneux, Comparison of toxic and teratogenic effects of *Lupinus formosus, L. arbustus and L. caudatus* in goats, J. Nat. Toxins 3 (1994) 83–93.
[34] K.E. Panter, L.F. James, D.R. Gardner, Lupines, poison-hemlock and *Nicotiana* spp: toxicity and teratogenicity in livestock, J. Nat. Toxins 8 (1999) 117–134.
[35] G.A. Sheveleva, The influence of smoking and nicotine on reproductive function, Akush. Ginekol. (USSR) 12 (1987) 46–51.
[36] D.N. Sims, R. James, T. Christensen, Another death due to ingestion of *Nicotiana glauca*, J. Forensic Sci. 44 (1999) 447–449.
[37] P.A. Steenkamp, F.R. van Heerden, B.-E. van Wyk, Accidental fatal poisoning by *Nicotiana glauca*: identification of anabasine by high performance liquid chromatography/photodiode array/mass spectrometry, Forensic Sci. Int. 127 (2002) 208–217.
[38] D.G. Upshall, Correlation of chick embryo teratogenicity with the nicotinic activity of a series of tetrahydropyrimidines, Teratology 5 (1972) 287–294.
[39] J. Weinzweig, K.E. Panter, M. Pantaloni, A. Spangenberger, J.S. Harper, F. Lui, D. Gardner, T.L. Wierenga, L.E. Edstrom, The fetal cleft palate: I. Characterization of a congenital model, Plast. Reconstr. Surg. 103 (1999) 419–428.
[40] J. Weinzweig, K.E. Panter, M. Pantaloni, A. Spangenberger, J. Harper, F. Lui, L.F. James, L.E. Edstrom, The fetal cleft palate: II. Scarless healing following in utero repair of a congenital model, Plast. Reconstr. Surg. 104 (1999) 1356–1364.
[41] J. Weinzweig, K.E. Panter, A. Spangenberger, J. Harper, R. McRae, L.E. Edstrom, The fetal cleft palate: III. Ultrasound and functional analysis of palatal development following in utero repair of the congenital model, Plast. Reconstr. Surg. 109 (2002) 2355–2362.
[42] J. Weinzweig, K.E. Panter, J. Seki, M. Pantaloni, A. Spangenberger, J.S. Harper, The fetal cleft palate: IV. Mid facial growth and bony development following in utero and neonatal repair of the congenitial caprine model, Plast. Reconstr. Surg. (submitted for publication).
[43] J.W. Wheeler, O. Olubajo, C.B. Storm, R.M. Duffield, Anabaseine: venom alkaloid of *Aphaenogaster* ants, Science 211 (1981) 1051–1052.